Joint ranging and phase offset estimation of multiple aviation vehicles using secondary radar

Mohammadkarimi, Mostafa; Leus, Geert; Rajan, Raj Thilak

DOI
10.1109/ICASSP48485.2024.10446219

Publication date
2024

Document Version
Final published version

Published in
2024 IEEE International Conference on Acoustics, Speech, and Signal Processing, ICASSP 2024 - Proceedings

Citation (APA)
Mohammadkarimi, M., Leus, G., & Rajan, R. T. (2024). Joint ranging and phase offset estimation of multiple aviation vehicles using secondary radar. In *2024 IEEE International Conference on Acoustics, Speech, and Signal Processing, ICASSP 2024 - Proceedings* (pp. 9131-9135). (ICASSP, IEEE International Conference on Acoustics, Speech and Signal Processing - Proceedings). IEEE. https://doi.org/10.1109/ICASSP48485.2024.10446219

ICASSP 2024 - 2024 IEEE International Conference on Acoustics, Speech and Signal Processing (ICASSP) | 979-8-3503-4485-1/24/$31.00 ©2024 IEEE | DOI: 10.1109/ICASSP48485.2024.10446219

JOINT RANGING AND PHASE OFFSET ESTIMATION OF MULTIPLE AVIATION VEHICLES USING SECONDARY RADAR

Mostafa Mohammadkarimi, Geert Leus, and Raj Thilak Rajan

Faculty of Electrical Engineering, Mathematics and Computer Science, Delft University of Technology

ABSTRACT

In this paper, we propose a new method for joint ranging and Phase Offset (PO) estimation of multiple transponder-equipped aviation vehicles (TEAVs), including Manned Aerial Vehicles (MAVs) and Unmanned Aerial Vehicles (UAVs). The proposed method employs the overlapping uncoordinated Automatic Dependent Surveillance–Broadcast (ADS-B) packets broadcasted by the TEAVs for joint range and PO estimation prior to ADS-B packet decoding; thus, it can improve air safety when packet decoding is infeasible due to packet collision. Moreover, it enables coherent detection of ADS-B packets, which can result in more reliable multiple target tracking in aviation systems using cooperative sensors for sense and avoid. By minimizing the Kullback–Leibler Divergence (KLD), we show that the received complex baseband signal, coming from K uncoordinated TEAVs, which is corrupted by Additive White Gaussian Noise (AWGN) at a single antenna receiver can be approximated by an independent and identically distributed (i.i.d.) Gaussian Mixture (GM) with 2^K mixture components in the two-dimensional plane. The proposed estimator employs the Expectation–Maximization (EM) algorithm to estimate the modes of the 2D Gaussian mixture followed by a reordering estimation technique to jointly estimate range and PO. Simulation results show that the proposed joint estimator outperforms excising methods, such as the time segmentation method and the blind adaptive beamforming.

Index Terms— Ranging, phase offset, cooperative navigation, expectation–maximization, ADS-B, UAV.

1. INTRODUCTION

Automatic Dependent Surveillance–Broadcast (ADS-B) is considered a promising solution to enable safe autonomous navigation of transponder-equipped aviation vehicles (TEAVs), including Unmanned Aerial Vehicles (UAVs), especially in urban environments [1]. In this solution, TEAVs are equipped with Global Positioning System (GPS) and a transponder and they broadcast their position information, which can be employed by the surrounding TEAVs to maintain a safe operation distance at low altitude and congested airspace.

One of the main challenges in the employment of a cooperative sensor system, such as ADS-B, is packet collisions due to a larger number of TEAVs. As the number of TEAVs in the airspace increases, the probability of packet collision also increases. The ADS-B system in its current form cannot handle packet collision; thus, a large number of packets are lost. Packet loss means less information and more uncertainty for the surrounding TEAVs, resulting in less air safety [2, 3].

Existing solutions for the separation of the overlapping ADS-B packets can be broadly divided into time-domain and spatial-domain methods [4–12]. These methods first separate the ADS-B packets. Then, by using the separated packets, they can estimate the range and Phase Offset (PO) of the TEAVs. The main issue with the above mentioned methods is that most of them can only separate two overlapping ADS-B signals [4, 5]. In this paper, we propose the Expectation–Maximization (EM)-based joint ranging and PO estimation algorithm for multiple ADS-B overlapping signals.

2. SYSTEM MODEL

We assume that K TEAVs asynchronously broadcast their ADS-B packets every T_{P} seconds and consider an observation window of length $T_{\mathrm{w}} = T_{\mathrm{P}}$ (Fig. 1a). To make the joint ranging and PO estimation independent of the arrival time of the ADS-B packets at the receiver, we approximate the received samples in the observation interval by an independent and identically distributed (i.i.d.) complex random variable as will be explained in Section 3. Hence, without loss of generality, we can consider the ADS-B packet reception in Fig. 1b to simplify modeling of the joint range and PO estimation. In this case, it is assumed that the ADS-B packet of the kth TEAV with a packet length of T_{A} is received at the receiver with an unknown time delay $\tau_k \in [0, \tau_{\max}]$ which is random in each observation window of length $T_{\mathrm{w}} = T_{\mathrm{P}}$. Here, $\tau_{\max} = T_{\mathrm{P}} - T_{\mathrm{A}}$ is the maximum time delay of a packet. For a baseband low pass filter with sufficient bandwidth B at the receiver, the received baseband signal is given by

$$y(t) \approx \sum_{k=1}^{K} \sqrt{P_k L_k}\, x_k(t - \tau_k) e^{j(2\pi \Delta f_k t + \theta_k)} + w(t), \quad (1)$$

where $t \in [0, T_{\mathrm{w}}]$, and where P_k, $x_k(t)$, $w(t)$, and L_k denote, the transmit power by the kth TEAV, the transmit Pulse Position Modulation (PPM) waveform by the kth TEAV, the additive noise with Power Spectral Density (PSD) N_0 over the bandwidth of the low pass filter $f \in [-B, B]$, and the path loss between the kth TEAV and the receiver, respectively. For free-space path loss, we have $L_k \triangleq \left(\lambda_{\mathrm{c}}/4\pi r_k\right)^2$, where r_k is the range between the kth TEAV and the receiver,

This work is partially funded by the European Leadership Joint Undertaking (ECSEL JU), under grant agreement No 876019, and the ADACORSA project - “Airborne Data Collection on Resilient System Architectures”. A part of this work has been accepted in IEEE TVT.

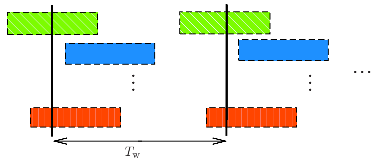

(a) The received ADS-B packet and the observation window with length T_w.

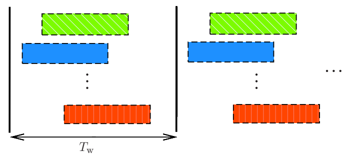

(b) A special case where the complete ADS-B packets of all TEAVs fall inside the observation window.

Fig. 1: The reception of the ADS-B packets at the receiver. Different colors are used to show the packet of TEAVs.

$\lambda_\mathrm{c} \triangleq c/f_\mathrm{c}$ is the wavelength of the carrier wave, and c denotes the speed of light, and f_c represents the carrier frequency. In (1), Δf_k and θ_k denote the carrier frequency offset and the PO of the kth TEAV. Since the ADS-B packets are short, we can consider that $\Delta f_k T_\mathrm{w} \ll 1$ and $\exp(j2\pi\Delta f_k t) \approx 1$ for $t \in [0, T_\mathrm{w}]$, $k = 1, 2, \cdots, K$. We assume that P_k is known at the receiver, and that $P_1 L_1 > P_2 L_2 > \ldots, P_K L_K$.

A sampling rate of $f_s \triangleq \frac{1}{T_\mathrm{s}} = 2\mathrm{M}$ samples/s is sufficient to capture the bit transitions of PPM signaling. Thus, the discrete-time received baseband signal after sampling, i.e., $y_n \triangleq y(nT_\mathrm{s})$, $n = 0, 1, \ldots, N$, where $N = 239 + M$, $M \triangleq \lfloor \frac{\tau_{\max}}{T_\mathrm{s}} \rfloor$, can be written in vector form as

$$\mathbf{y} = \sum_{k=1}^{K} h_k \mathbf{x}_k + \mathbf{w} = \sum_{k=1}^{K} \mathbf{z}_k + \mathbf{w} = \mathbf{g} + \mathbf{w}, \tag{2}$$

with $\mathbf{g} = \begin{bmatrix} g_0 & \ldots & g_N \end{bmatrix}^T = \sum_{k=1}^{K} \mathbf{z}_k$, $\mathbf{z}_k \triangleq \begin{bmatrix} z_{k,0} & \cdots & z_{k,N} \end{bmatrix}^T = h_k \mathbf{x}_k$, $\mathbf{y} \triangleq \begin{bmatrix} y_0 & \ldots & y_N \end{bmatrix}^T$, $\mathbf{w} \triangleq \begin{bmatrix} w_0 & \ldots & w_N \end{bmatrix}^T$, $w_n \triangleq w(nT_\mathrm{s})$, $h_k \triangleq \beta_k e^{j\theta_k}$, $\beta_k \triangleq \sqrt{P_k L_k}$, and

$$\mathbf{x}_k \triangleq \begin{bmatrix} x_{k,0} \ x_{k,1} & \cdots & x_{k,N} \end{bmatrix}^T \triangleq \begin{bmatrix} \mathbf{0}_{m_k}^T \ \mathbf{s}^T \ \mathbf{d}_k^T \ \mathbf{0}_{M-m_k}^T \end{bmatrix}^T. \tag{3}$$

In (3), $x_{k,n} \triangleq x_k(nT_\mathrm{s} - \tau_k)$, $\mathbf{d}_k \in \{0, 1\}^{224}$, is the PPM data vector of the kth TEAV with a length of 224 symbols, $\mathbf{s} \in \{0, 1\}^{16}$ is the preamble vector of size 16, and $M \triangleq \lfloor \frac{\tau_{\max}}{T_\mathrm{s}} \rfloor$ and $m_k \triangleq \lfloor \frac{\tau_k}{T_\mathrm{s}} \rfloor$ denote the maximum possible integer delay for a TEAV and the integer delay of the kth TEAV, respectively. The integer delays m_k, $k = 1, 2, \cdots, K$, are unknown at the receiver and their values change from one observation window to another. The vector $\mathbf{w}$ in (2) denotes the Additive White Gaussian Noise (AWGN) with covariance matrix $\mathbb{E}\{\mathbf{w}\mathbf{w}^T\} = \sigma_\mathrm{w}^2 \mathbf{I} = 2N_0 B \mathbf{I}$. We define hypothesis H_m^k as

$$H_m^k: \quad \mathbf{x}_k = \begin{bmatrix} \mathbf{0}_m^T, \mathbf{s}^T, \mathbf{d}_k^T, \mathbf{0}_{M-m}^T \end{bmatrix}^T, \tag{4}$$

which represents the ADS-B packet of the kth TEAV arriving at the receiver with integer delay $m_k = m \in \{0, 1, \ldots, M\}$.

3. DISTRIBUTION APPROXIMATION

To remove the dependency of joint ranging and PO estimation from the unknown arrival time of the ADS-B packets at the receiver, i.e., m_k, we approximate the received noisy samples.

Theorem 1. *By maximizing the KLD criterion, the elements of the ADS-B packet of the kth TEAV, i.e., $\mathbf{x}_k = [x_{k,0} \ x_{k,1} \ \ldots \ x_{k,N}]^T = \begin{bmatrix} \mathbf{0}_{m_k}^T \ \mathbf{s}^T \ \mathbf{d}_k^T \ \mathbf{0}_{M-m_k}^T \end{bmatrix}^T$ can be approximated by an i.i.d. random variable that are Bernoulli distributed with parameter $p = (M + 124)/(M + 240)$ and Probability Mass Function (PMF) as (proof in [13])*

$$q(x; p) = \begin{cases} p & \text{if } x = 0, \\ 1 - p & \text{if } x = 1. \end{cases} \tag{5}$$

Since $\mathbf{z}_k = h_k \mathbf{x}_k$ is the scaled version of $\mathbf{x}_k$, and p is independent of m_k, the elements of the complex vector $\mathbf{z}_k$ can be approximated by i.i.d. complex random variables Z_k with Probability Density Function (PDF) $f_{Z_k}\big(z; p, h_k\big)$ as follows

$$f_{Z_k}\big(z; p, h_k\big) = p\delta_\mathrm{c}(z) + (1 - p)\delta_\mathrm{c}(z - h_k), \tag{6}$$

where $\delta_\mathrm{c}(z)$, $z = z_\mathrm{r} + jz_\mathrm{I} \in \mathbb{C}$, is the complex Delta function and is defined as $\delta_\mathrm{c}(z) \triangleq \delta(z_\mathrm{r})\delta(z_\mathrm{I})$, with $\delta(t)$, $t \in \mathbb{R}$ as the Dirac Delta function.

We consider that $g_i \triangleq \sum_{k=1}^{K} z_{k,i} \sim G$ and $z_{k,i} \sim Z_k$ given in (6), where the symbol $\sim$ denotes distributed according to. The PDF of the sum of independent random variables is obtained as the convolution of the PDFs. For the complex random variable, $G = \sum_{k=1}^{K} Z_k$, by employing the multi-binomial theorem [14], we can obtain the PDF of G as [13]

$$f_G(g; p, \mathbf{h}) = \sum_{v_1=0}^{1} \cdots \sum_{v_K=0}^{1} \Bigg[p^{\sum_{k=1}^{K} v_k} (1 - p)^{K - \sum_{k=1}^{K} v_k} \times \delta_\mathrm{c}\Big(g - \sum_{k=1}^{K} (1 - v_k) h_k \Big) \Bigg], \tag{7}$$

where $\mathbf{h} \triangleq [h_1, h_2, \cdots, h_K]^T$. For the circularly symmetric complex Gaussian noise vector, $\mathbf{w}$, the PDF of the random variable W associated with the noise elements is expressed as

$$f_W(w; \sigma_\mathrm{w}^2) \triangleq \frac{1}{\pi\sigma_\mathrm{w}^2} \exp\left(\frac{-|w|^2}{\sigma_\mathrm{w}^2} \right), \tag{8}$$

where $w \in \mathbb{C}$. From (2), we have $y_n = g_n + w_n$, $n = 0, 1, \ldots, N$, where $g_n \sim G$ and $w_n \sim W$. Since G and W are independent complex random variables, the PDF of $Y = G + W$ is obtained by the linear convolution of the PDFs in (7) and (8), which results in

$$f_Y(y; p, \boldsymbol{\beta}, \boldsymbol{\theta}, \sigma_\mathrm{w}^2) = \sum_{a=0}^{2^K - 1} \frac{\xi_a}{\pi\sigma_\mathrm{w}^2} \exp\left(- \frac{|y - \mu_a|^2}{\sigma_\mathrm{w}^2} \right), \tag{9}$$

where $\boldsymbol{\beta} \triangleq \begin{bmatrix} \beta_1 \ \beta_2 & \ldots & \beta_K \end{bmatrix}^T$, $\boldsymbol{\theta} \triangleq \begin{bmatrix} \theta_1 \ \theta_2 & \ldots & \theta_K \end{bmatrix}^T$, $\xi_a \triangleq p^{\sum_{k=1}^{K} b_k} (1 - p)^{K - \sum_{k=1}^{K} b_k}$, and

$$\mu_a \triangleq \sum_{k=1}^{K} (1 - b_k) h_k = \sum_{k=1}^{K} (1 - b_k) \beta_k \exp(j\theta_k) \tag{10}$$

with b_i the ith bit in the binary representation of $a = (b_K, b_{K-1}, \ldots, b_1)_2$, $b_i \in \{0, 1\}$, and $a = 0, 1, \ldots, 2^K - 1$. As seen, $f_Y(y; p, \boldsymbol{\beta}, \boldsymbol{\theta}, \sigma_{\mathrm{w}}^2)$ represents a 2D Gaussian Mixture (GM), where its modes are located at the delta functions given in (7).

4. JOINT RANGE AND PO ESTIMATION

The Maximum Likelihood Estimation (MLE) for the vector parameters $[\boldsymbol{\beta}^T \ \boldsymbol{\theta}^T]^T$ given observation vector $\mathbf{y} = [y_0 \, y_2 \ \ldots \ y_N]^T$ is expressed as

$$\{\hat{\boldsymbol{\beta}}, \hat{\boldsymbol{\theta}}\} = \arg\max_{\boldsymbol{\beta}, \boldsymbol{\theta}} \sum_{n=0}^{N} \ln f_Y(y_n; p, \boldsymbol{\beta}, \boldsymbol{\theta}, \sigma_{\mathrm{w}}^2). \tag{11}$$

The MLE in (11) cannot be analytically obtained in a trackable manner. An alternative solution is to employ the EM algorithm to estimate the 2^K modes of the GM; then, we can decouple the desired parameters, i.e., $\boldsymbol{\beta}$ and $\boldsymbol{\theta}$ from the estimated modes. Let $\boldsymbol{\mu} \triangleq [\mu_0 \, \mu_1 \ \ldots \ \mu_{2^K-1}]^T$ denote the mode vector of the GM, where μ_a, $a = 0, 1, \ldots, 2^K - 1$, is given by (10). Let us define the discrete function $\chi_q(n)$ as

$$\chi_q(n) : \{1, 2, \ldots, l\} \longrightarrow \{1, 2, \ldots, l\}, \tag{12}$$

where for $n_1 \neq n_2$, $\chi_q(n_1) \neq \chi_q(n_2)$. There are $Q_l \triangleq l!$ unique functions in the form of (12), where ! denotes the factorial function. Using (12), Q_l permutation matrices of size $l \times l$ can be defined as

$$\boldsymbol{\Lambda}_q = \left[\mathbf{e}_{\chi_q(1)}^T \, \mathbf{e}_{\chi_q(2)}^T \ \ldots \ \mathbf{e}_{\chi_q(l)}^T\right]^T, \tag{13}$$

where $\mathbf{e}_\ell$, $\ell = 1, 2, \ldots, l$, denote the standard basis vectors of length l with a 1 in the ℓth coordinate and 0's elsewhere. The set composed of all permutations of vector $\mathbf{a} = [a_1 \ a_2 \ \ldots \ a_l]^T$ is given by

$$\mathcal{F}_{\mathbf{a}}^{Q_l} \triangleq \left\{\boldsymbol{\Lambda}_1\mathbf{a}, \boldsymbol{\Lambda}_2\mathbf{a}, \ldots, \boldsymbol{\Lambda}_{Q_l}\mathbf{a}\right\}. \tag{14}$$

The EM algorithm estimates the permuted mode vector $\boldsymbol{\eta} = [\eta_0 \, \eta_1 \ \ldots \eta_{2^K-1}]^T \in \mathcal{F}_{\boldsymbol{\mu}}^{Q_{2^K}} \subset \mathbb{C}^{2^K}$, where $Q_{2^K} = 2^K!$ and $\boldsymbol{\mu} \triangleq [\mu_0 \ \mu_1 \ \ldots \ \mu_{2^K-1}]^T$. The EM algorithm defines a latent random vector $\mathbf{u} \triangleq [u_0 \ u_1 \ \ldots \ u_N]^T$ that determines the GM component from which the observation originates, i.e., $f_{Y|U}(y_n | u_n = a; p, \boldsymbol{\beta}, \boldsymbol{\theta}, \sigma_{\mathrm{w}}^2) \sim \mathcal{CN}(y_n; \mu_a, \sigma_{\mathrm{w}}^2)$, where $P_U(u_n = a) = \xi_a$ for $n = 0, 1, \ldots, N$ and $a = 0, 1, \ldots, 2^K - 1$. The EM algorithm iteratively maximizes the expected value of the complete-data log-likelihood function to estimate the permuted mode vector $\boldsymbol{\eta} = [\eta_0 \, \eta_1 \ \ldots \eta_{2^K-1}]^T \in \mathcal{F}_{\boldsymbol{\mu}}^{Q_{2^K}} \subset \mathbb{C}^{2^K}$ of the GM as follows [15]

$$\hat{\boldsymbol{\eta}}^{(t+1)} = \arg\max_{\boldsymbol{\eta}} Q(\boldsymbol{\eta} | \boldsymbol{\eta}^{(t)}), \tag{15}$$

where $\boldsymbol{\eta}^{(0)}$ is the initialization vector,

$$\begin{aligned} Q(\boldsymbol{\eta}|\boldsymbol{\eta}^{(t)}) &= \mathbb{E}_{\boldsymbol{U}|\boldsymbol{Y}, \boldsymbol{\eta}^{(t)}}\Big\{\ln f_{\boldsymbol{Y}, \boldsymbol{U}}(\mathbf{y}, \mathbf{u}; p, \boldsymbol{\eta}, \sigma_{\mathrm{w}}^2)\Big\} \qquad (16) \\ &= \sum_{n=0}^{N} \sum_{a=0}^{2^K-1} \lambda_{a,n}^{(t)} \left(\ln \frac{\xi_a}{\pi \sigma_{\mathrm{w}}^2} - \frac{|y_n - \eta_a|^2}{\sigma_{\mathrm{w}}^2}\right), \end{aligned}$$

with

$$\begin{aligned} \lambda_{a,n}^{(t)} &= P_{U|Y}\big(u_n = a | y_n; \boldsymbol{\eta}^{(t)}\big) \qquad (17) \\ &= \frac{\xi_a \mathcal{CN}\big(y_n; \eta_a^{(t)}, \sigma_{\mathrm{w}}^2\big)}{\sum_{q=0}^{2^K-1} \xi_q \mathcal{CN}\big(y_n; \eta_q^{(t)}, \sigma_{\mathrm{w}}^2\big)}, \end{aligned}$$

and the complete-data likelihood function is given by

$$f_{\boldsymbol{Y}, \boldsymbol{U}}(\mathbf{y}, \mathbf{u}; p, \boldsymbol{\eta}, \sigma_{\mathrm{w}}^2) = \prod_{n=0}^{N} \prod_{a=0}^{2^K-1} \big(\xi_a \mathcal{CN}(y_n; \eta_a, \sigma_{\mathrm{w}}^2)\big)^{\mathbb{I}\{u_n = a\}}.$$

In above equation, $\mathbb{I}\{\cdot\}$ denotes the indicator function, and ξ_a is a function of $p = (M + 124)/(M + 240)$. The EM algorithm at the $(t+1)$th iteration estimates the vector $\boldsymbol{\eta}^{(t+1)} = [\eta_0^{(t+1)} \ \eta_1^{(t+1)} \ \ldots \eta_{2^K-1}^{(t+1)}]^T$ which is a permuted version of the vector $\boldsymbol{\mu}$. The order of $\boldsymbol{\eta}^{(t+1)}$ depends on the initialization of the EM algorithm, i.e., $\boldsymbol{\eta}^{(0)}$. By solving the maximization problem in (15), the elements of $\boldsymbol{\eta}^{(t+1)}$ are updated as

$$\eta_a^{(t+1)} = \frac{\sum_{n=0}^{N} \lambda_{a,n}^{(t)} y_n}{\sum_{n=0}^{N} \lambda_{a,n}^{(t)}}, \tag{18}$$

for $a = 0, 1, \ldots, 2^K - 1$, where the convergence condition for the EM algorithm is $\|\boldsymbol{\eta}^{(t+1)} - \boldsymbol{\eta}^{(t)}\| < \epsilon$, with ϵ a preset threshold. We denote $\hat{\boldsymbol{\eta}} = \boldsymbol{\eta}^{(t+1)}$ when the EM algorithm converges at the $(t+1)$th iteration.

5. REORDERING ESTIMATION

The goal of reordering estimation is to change the order of the elements in $\hat{\boldsymbol{\eta}} \triangleq [\hat{\eta}_0 \ \hat{\eta}_1 \ \ldots \ \hat{\eta}_{2^K-1}]^T$, obtained by the EM algorithm, to achieve a new vector $\hat{\boldsymbol{\mu}} \triangleq [\hat{\mu}_0 \ \hat{\mu}_1 \ \ldots \ \hat{\mu}_{2^K-1}]^T$ that corresponds to an estimate of $\boldsymbol{\mu} \triangleq [\mu_0 \ \mu_1 \ \ldots \ \mu_{2^K-1}]^T$. Let us denote $\hat{\eta}_i$ as the element of $\hat{\boldsymbol{\eta}}$ that corresponds to $\mu_{2^K-1} = 0$. The index i can be estimated as

$$|\hat{\eta}_i| < \min\Big\{|\hat{\eta}_0|, |\hat{\eta}_1|, \ldots, |\hat{\eta}_{i-1}|, |\hat{\eta}_{i+1}|, \ldots, |\hat{\eta}_{2^K-1}|\Big\}. \tag{19}$$

Accordingly, we have $\hat{\mu}_{2^K-1} = \hat{\eta}_i$. Let us now define

$$\hat{\boldsymbol{\eta}}_i \triangleq [\hat{\eta}_0 \ \hat{\eta}_1 \ \ldots \ \hat{\eta}_{i-1} \ \hat{\eta}_{i+1} \ \ldots \ \hat{\eta}_{2^K-1}]^T, \tag{20}$$

and

$$\begin{aligned} \hat{\mathcal{A}}_l \triangleq \Big\{ &[\phi_1 \ \phi_2 \ \ldots \ \phi_l]^T \big| \forall d \in \{1, 2, \ldots, l\}, \\ &\phi_d \in \{\hat{\eta}_0, \hat{\eta}_1, \ldots \ \hat{\eta}_{i-1}, \hat{\eta}_{i+1} \ \ldots \ \hat{\eta}_{2^K-1}\}, \qquad (21) \\ &|\phi_1| > |\phi_2| > \ldots |\phi_l| \Big\}. \end{aligned}$$

In [13], we propose different reordering estimation methods for $\hat{\boldsymbol{\beta}}$ and $\hat{\boldsymbol{\theta}}$. The Least Squares (LS) reordering estimation for $\hat{\boldsymbol{\beta}}$ and $\hat{\boldsymbol{\theta}}$ form $\hat{\boldsymbol{\eta}}_i$ is given by

$$\hat{\mathbf{h}} = \hat{\boldsymbol{\beta}} e^{j\hat{\boldsymbol{\theta}}} = \hat{\boldsymbol{\Lambda}} \mathbf{A} \hat{\boldsymbol{\Phi}}, \tag{22}$$

where

$$\{\hat{\mathbf{\Lambda}}, \hat{\mathbf{\Phi}}\} = \underset{\mathbf{\Lambda},\mathbf{\Phi}}{\arg\min} \left\|\mathbf{\Lambda}\mathbf{A}\mathbf{\Phi} - \hat{\boldsymbol{\eta}}_i\right\|_2, \tag{23}$$
$$\text{s.t. } \mathbf{\Phi} \triangleq [\Phi_1, \Phi_2, \ldots, \Phi_K]^T \in \hat{\mathcal{A}}_K$$
$$\mathbf{\Lambda} \in \{\mathbf{\Lambda}_1, \mathbf{\Lambda}_2, \ldots, \mathbf{\Lambda}_{(2^{K-1})!}\}$$

where $\mathbf{\Lambda}_i$ is a permutation matrix of size $2^{K-1} \times 2^{K-1}$ given in (13) for $l = 2^{K-1}$, and $\mathbf{A}$ is the $2^{K-1} \times K$ matrix as $\mathbf{A} \triangleq \left[\mathbf{e}_1\, \mathbf{e}_2\, \ldots\, \mathbf{e}_K\, \mathbf{e}_1\!+\!\mathbf{e}_2\, \mathbf{e}_1\!+\!\mathbf{e}_3 \ldots\, \mathbf{e}_1\!+\!\mathbf{e}_2\!+\!\ldots\!+\!\mathbf{e}_K\right]^T$, where $\mathbf{e}_j$, $j = 1, 2, \ldots, K$, denote the standard basis vectors of length K.

Joint Range and PO Estimation: For joint range and PO estimation of K TEAVs, the modes $\mu_{a_k} \triangleq \sqrt{P_k L_k} e^{j\theta_k}$, $k = 1, 2, \ldots, K$, are needed to be estimated, where

$$a_k = \sum_{\substack{n=0 \\ n \neq k-1}}^{K-1} 2^n. \tag{24}$$

Let $\hat{\mu}_{a_k}$, $k = 1, 2, \ldots, K$, denote the estimated modes after reordering estimation. By using $L_k \triangleq \left(\lambda_c / 4\pi r_k\right)^2$, the range and PO for the kth TEAV are estimated as

$$\hat{r}_k = \frac{\lambda_c \sqrt{P_k}}{\left|4\pi\hat{\mu}_{a_k}\right|}, \tag{25}$$

and

$$\hat{\theta}_k = \begin{cases} \tan^{-1}\frac{\Im\{\hat{\mu}_{a_k}\}}{\Re\{\hat{\mu}_{a_k}\}}, & \Re\{\hat{\mu}_{a_k}\} \geq 0 \\ \tan^{-1}\frac{\Im\{\hat{\mu}_{a_k}\}}{\Re\{\hat{\mu}_{a_k}\}} + \pi, & \Re\{\hat{\mu}_{a_k}\} < 0, \end{cases} \tag{26}$$

where $\Im\{\cdot\}$ and $\Re\{\cdot\}$ are the real and imaginary operators.

6. MULTIPLE ANTENNAS RECEIVER

We consider N_r single antenna receivers. With the assumption that the path loss between the kth TEAV and the ℓth receive antenna is the same for all receive antennas, i.e, $L_{\ell,k} = L_k$, $k = 1, 2, \ldots, K$, $\ell = 1, 2, \ldots, N_r$, the received complex baseband signal at the multiple-receive antennas is given by

$$\mathbf{Y} = \mathbf{H}\mathbf{X} + \mathbf{W}, \tag{27}$$

where $\mathbf{X} \triangleq [\mathbf{x}_1\, \ldots\, \mathbf{x}_K]^T \in \mathbb{C}^{K\times(N+1)}$, $\mathbf{Y} \triangleq [\mathbf{y}_0 \ldots \mathbf{y}_N] \in \mathbb{C}^{N_r\times(N+1)}$, $\mathbf{x}_k$ is given by (3), and $\mathbf{y}_n \triangleq [y_{1,n}\, \ldots\, y_{N_r,n}]^T$ denotes the received vector at time index n. In (27), the matrices $\mathbf{H} \in \mathbb{C}^{N_r\times K}$ and $\mathbf{W} \in \mathbb{C}^{N_r\times(N+1)}$ are given as $\mathbf{H} = [\mathbf{h}_1\, \ldots\, \mathbf{h}_{N_r}]^T$ and $\mathbf{W} = [\mathbf{w}_1\, \ldots\, \mathbf{w}_{N_r}]^T$, where $\mathbf{h}_\ell \triangleq \left[h_{\ell,1}\, \ldots\, h_{\ell,K}\right]^T = \left[\beta_1 \exp(j\theta_{\ell,1})\, \ldots\, \beta_N \exp(j\theta_{\ell,K})\right]^T$, $\beta_k = \beta_{\ell,k} = \sqrt{P_k L_k}$, $\mathbf{w}_\ell \triangleq [w_{\ell,0}\, w_{\ell,1}\, \ldots\, w_{\ell,N}]^T$ with $w_{\ell,n} \sim \mathcal{CN}(0, \sigma_w^2)$ the complex Gaussian noise at the ℓth receive antenna at time index n. As seen, while $\beta_{1,k} = \beta_{2,k} = \cdots = \beta_{N_r,k} = \beta_k$, the phases $\theta_{1,k}, \theta_{2,k}, \ldots, \theta_{N_r,k}$ are independent random values in $[0\; 2\pi)$ [13].

The joint PDF of the elements of $\mathbf{Y}$ is given by $f_{\mathbf{Y}}(\mathbf{Y}; p, \boldsymbol{\beta}, \mathbf{\Theta}, \sigma_w^2) = \prod_{\ell=1}^{N_r}\prod_{n=0}^{N} f_Y(y_{\ell,n}; p, \boldsymbol{\beta}, \boldsymbol{\theta}_\ell, \sigma_w^2)$, where $\boldsymbol{\beta} \triangleq [\beta_1\, \ldots\, \beta_K]^T$, $\mathbf{\Theta} \triangleq \left[\boldsymbol{\theta}_1^T\, \ldots\, \boldsymbol{\theta}_{N_r}^T\right]^T$, $\boldsymbol{\theta}_\ell \triangleq \left[\theta_{\ell,1}\, \ldots\, \theta_{\ell,K}\right]^T$, and $f_Y(y; p, \boldsymbol{\beta}, \boldsymbol{\theta}, \sigma_w^2)$ is given in (9). Analogous to the single receive antenna scenario, we can employ the EM algorithm for estimating the modes of the GM for each receive antenna. While the EM algorithm estimates $N_r 2^K$ parameters, only $N_r K$ parameters are used for joint ranging and PO estimation of K TEAVs. These $N_r K$ modes are $\mu_{\ell,a_1}, \mu_{\ell,a_2}, \ldots, \mu_{\ell,a_K}$, where a_k is defined in (24). After the EM converges, each receive antenna independently applies estimation mapping as explained in section 5. Let $\hat{\mu}_{\ell,a_1}, \hat{\mu}_{\ell,a_2}, \ldots, \hat{\mu}_{\ell,a_K}$ denote the estimated and reordered modes at the ℓth receive antenna. By averaging, we can write $|\hat{\mu}_{a_k}| = \frac{1}{N_r}\sum_{\ell=1}^{N_r}|\hat{\mu}_{\ell,a_k}| \propto \frac{1}{\hat{r}_k}$, where $k = 1, 2, \ldots, K$. By substituting $|\hat{\mu}_{a_k}|$ into (25), we can estimate the range of the kth TEAV. The PO for each TEAV receive antenna is obtained by replacing $\hat{\mu}_{\ell,a_1}, \ldots, \hat{\mu}_{\ell,a_K}$, $\ell = 1, \cdots, N_r$ into (26) [13].

7. SIMULATION RESULTS

We considered $K = 2$ TEAVs with ranges $r_1, r_2 \in \mathcal{U}_c[1, 10]$ Km. The azimuth and elevation angles of the TEAVs are assumed to be $\theta_1, \theta_2 \in \mathcal{U}_c[-\pi, \pi)$ and $\psi_1, \psi_2 \in \mathcal{U}_c[0, \pi/2]$, respectively. The number of receive antennas was set to $N_r = 5$. The details on the simulation setup is given in [13].

Fig. 2 compares the probabilistic performance (defined in [13]) of the EM-based estimator with the time segmentation (TS) and the blind adaptive beamforming (BAB) ADS-B packet separation methods in [4] and [5] for $B = 36$ MHz. We also show the performance of the Cramer-Rao Lower Bound (CRLB). As seen, our method outperforms the TS and the BAB methods since it employs all the observation samples including the overlapping snapshot for ranging and PO estimation; however, the TS and the BAB methods rely on the non-overlapping snapshot for ADS-B packet recovery.

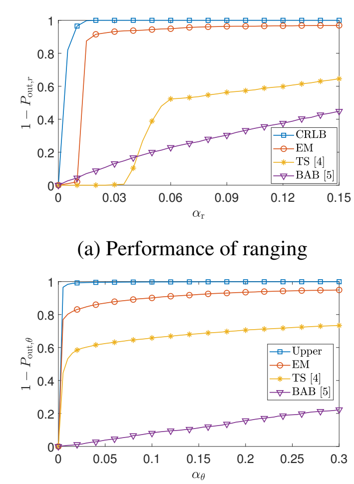

(a) Performance of ranging

(b) Performance of PO estimation

Fig. 2: Performance comparison of the proposed EM-based joint ranging and PO estimator for $K = 2$ TEAVs and $N_r = 5$.

8. REFERENCES

[1] P. Angelov, *Sense and avoid in UAS: research and applications*. John Wiley & Sons, 2012.

[2] M. Strohmeier, M. Schäfer, V. Lenders, and I. Martinovic, "Realities and challenges of nextgen air traffic management: the case of ADS-B," *IEEE Commun. Mag.*, vol. 52, no. 5, pp. 111–118, May 2014.

[3] Y. Kim, J.-Y. Jo, and S. Lee, "ADS-B vulnerabilities and a security solution with a timestamp," *IEEE Aerosp. Electron. Syst. Mag.*, vol. 32, no. 11, pp. 52–61, Nov. 2017.

[4] K. Li, J. Kang, H. Ren, and Q. Wu, "A reliable separation algorithm of ADS-B signal based on time domain," *IEEE Access*, vol. 9, pp. 88 019–88 026, May 2021.

[5] W. Wang, R. Wu, and J. Liang, "ADS-B signal separation based on blind adaptive beamforming," *IEEE Trans. Veh. Technol.*, vol. 68, no. 7, pp. 6547–6556, May 2019.

[6] Z. Zhang, "Optimization performance analysis of 1090ES ADS-B signal separation algorithm based on PCA and ICA," *International Journal of Performability Engineering*, vol. 14, no. 4, p. 741, 2018.

[7] M. Leonardi and M. Maisano, "Degarbling technique for low cost ADS-B receivers," in *proc. IEEE MetroAeroSpace*, Oct. 2019, pp. 65–69.

[8] Y. Bi and C. Li, "Multi-scale convolutional network for space-based ADS-B signal separation with single antenna," *Applied Sciences*, vol. 12, no. 17, p. 8816, Sept. 2022.

[9] W. Wang, J. Liu, and J. Liang, "Single antenna ADS-B overlapping signals separation based on deep learning," *Digital Signal Processing*, vol. 132, p. 103804, Nov. 2022.

[10] N. Petrochilos and A.-J. van der Veen, "Algorithms to separate overlapping secondary surveillance radar replies," in *proc. IEEE ISSPIT*, May 2004, pp. 17–21.

[11] L. Dan and C. Tao, "Single-antenna overlapped ADS-B signal self-detection and separation algorithm based on EMD," *J. Signal Process.*, vol. 35, no. 10, pp. 1680–1689, 2019.

[12] N. Petrochilos, G. Galati, L. Mené, and E. Piracci, "Separation of multiple secondary surveillance radar sources in a real environment by a novel projection algorithm," in *proc. IEEE ISSPIT*, Dec. 2005, pp. 125–130.

[13] M. Mohammadkarimi, G. Leus, and R. T. Rajan, "Joint ranging and phase offset estimation for multiple drones using ADS-B signatures," *IEEE Trans. Veh. Technol.*, pp. 1–15, Sept. 2023, DOI: 10.1109/TVT.2023.3318192.

[14] C. Morris, "Central limit theorems for multinomial sums," *The Annals of Statistics*, pp. 165–188, Jan. 1975.

[15] G. J. McLachlan, S. X. Lee, and S. I. Rathnayake, "Finite mixture models," *Annual review of statistics and its application*, vol. 6, pp. 355–378, 2019.